

Single Spin Asymmetry in Open Charm Photoproduction and Decay as a Test of pQCD

N.Ya. Ivanov*

Yerevan Physics Institute, Alikhanian Br.2, 0036 Yerevan, Armenia

P.E. Bosted[†] and S.E. Rock[‡]

University of Massachusetts, Amherst, Massachusetts 01003

K. Griffioen[§]

College of William and Mary, Williamsburg, Virginia 23187

We analyze the possibility of measuring the single spin asymmetry (SSA) in open charm production by linearly polarized photons in the planned E160/E161 experiments at SLAC using the inclusive spectra of secondary (decay) leptons. In leading order pQCD, the SSA in the azimuthal distribution of the charged decay lepton is predicted to be about 0.2 for SLAC kinematics. Our calculations show that the SSA in the decay lepton distribution is well defined in pQCD: it is stable both perturbatively and parametrically, and practically insensitive to theoretical uncertainties in the charm semileptonic decays. Nonperturbative contributions to the leptonic SSA due to the gluon transverse motion in the target, heavy quark fragmentation and Fermi motion of the c -quark inside the D -meson are predicted to be about 10%. We conclude that measurements of the azimuthal asymmetry in the secondary lepton distribution would provide a good test of the applicability of pQCD to open charm production at energies of fixed target experiments. Our analysis of the SLAC experimental conditions shows that this SSA can be measured in E160/E161 with an accuracy of about ten percent.

PACS numbers: 12.38.Bx, 13.88.+e, 13.85.Ni

Keywords: Perturbative QCD, Heavy Flavor Photoproduction, Single Spin Asymmetry

I. INTRODUCTION

In the framework of perturbative QCD, the basic spin-averaged characteristics of heavy flavor hadro-, photo- and electroproduction are known exactly up to the next-to-leading order (NLO). During the last ten years, these NLO results have been widely used for a phenomenological description of available data (for a review see [1]). At the same time, the key question remains open: How to test the applicability of QCD at fixed order to heavy quark production? The problem is twofold. On the one hand, the NLO corrections are large; they increase the leading order (LO) predictions for both charm and bottom production cross sections by approximately a factor of two. For this reason, one could expect that higher-order corrections, as well as nonperturbative contributions, can be essential, especially for the c -quark case. On the other hand, it is very difficult to compare pQCD predictions for spin-averaged cross sections with experimental data directly, without additional assumptions, because of a high sensitivity of the theoretical calculations to standard uncertainties in the input QCD parameters. The total uncertainties associated with the unknown values of the heavy quark mass, m_Q , the factorization and renormalization scales, μ_F and μ_R ,

*Electronic address: nikiv@yerphi.am

[†]Electronic address: bosted@slac.stanford.edu

[‡]Electronic address: ser@slac.stanford.edu

[§]Electronic address: griff@physics.wm.edu

Λ_{QCD} and the parton distribution functions are so large that one can only estimate the order of magnitude of the pQCD predictions for total cross sections at fixed target energies [2, 3].

In recent years, the role of higher-order corrections has been extensively investigated in the framework of the soft gluon resummation formalism. For a review see Ref.[4]. Formally resummed cross sections are ill-defined due to the Landau pole contribution, and a few prescriptions have been proposed to avoid the renormalon ambiguities [5–7]. Unfortunately, numerical predictions for the heavy quark production cross sections can depend significantly on the choice of resummation prescription [8]. Another open question, also closely related to convergence of the perturbative series, is the role of subleading contributions which are not, in principle, under control of the resummation procedure [8, 9].

For this reason, it is of special interest to study those observables that are well-defined in pQCD. A nontrivial example of such an observable is proposed in [10, 11], where the charm and bottom production by linearly polarized photons,

$$\gamma^\uparrow + N \rightarrow Q + X[\overline{Q}], \quad (1)$$

was considered¹. In particular, the single spin asymmetry (SSA) parameter, $A_Q(p_{QT})$, which measures the parallel-perpendicular asymmetry in the quark azimuthal distribution,

$$\frac{d^2\sigma_Q}{dp_{QT}d\varphi_Q}(p_{QT}, \varphi_Q) = \frac{1}{2\pi} \frac{d\sigma_Q^{\text{unp}}}{dp_{QT}}(p_{QT}) [1 + A_Q(p_{QT})\mathcal{P}_\gamma \cos 2\varphi_Q], \quad (2)$$

where

$$A_Q(p_{QT}) = \frac{1}{\mathcal{P}_\gamma} \frac{d^2\sigma_Q(p_{QT}, \varphi_Q = 0) - d^2\sigma_Q(p_{QT}, \varphi_Q = \pi/2)}{d^2\sigma_Q(p_{QT}, \varphi_Q = 0) + d^2\sigma_Q(p_{QT}, \varphi_Q = \pi/2)}, \quad (3)$$

has been calculated. In (2) and (3), $\frac{d\sigma_Q^{\text{unp}}}{dp_{QT}}$ is the unpolarized cross section, $d^2\sigma_Q(p_{QT}, \varphi_Q) = \frac{d^2\sigma_Q}{dp_{QT}d\varphi_Q}(p_{QT}, \varphi_Q)$, \mathcal{P}_γ is the degree of linear polarization of the incident photon beam and φ_Q is the angle between the beam polarization direction and the observed quark transverse momentum, p_{QT} . The following remarkable properties of the SSA, $A_Q(p_{QT})$, have been observed [10]:

- The azimuthal asymmetry (3) is of leading twist; in a wide kinematical region, it is predicted to be about 0.2 for both charm and bottom quark production.
- At energies sufficiently above the production threshold, the LO predictions for $A_Q(p_{QT})$ are insensitive (to within few percent) to uncertainties in the QCD input parameters.
- Nonperturbative corrections to the b -quark azimuthal asymmetry are negligible. Because of the smallness of the c -quark mass, the analogous corrections to $A_c(p_{QT})$ are larger; they are of the order of 20%.

In Ref. [11], radiative corrections to the integrated cross section,

$$\frac{d\sigma_Q}{d\varphi_Q}(S, \varphi_Q) = \frac{\sigma_Q^{\text{unp}}(S)}{2\pi} [1 + A_Q(S)\mathcal{P}_\gamma \cos 2\varphi_Q], \quad (4)$$

have been investigated in the soft-gluon approximation. (In Eq. (4), \sqrt{S} is the center-of-mass energy of the process (1)). Calculations [11] indicate a high perturbative stability of the pQCD predictions for $A_Q(S)$. In particular,

- At the next-to-leading logarithmic (NLL) level, the NLO and NNLO predictions for $A_Q(S)$ affect the LO results by less than 1% and 2%, respectively.

¹ The well-known examples are the shapes of differential cross sections of heavy flavor production which are sufficiently stable under radiative corrections.

- Computations of the higher order contributions (up to the 6th order in α_s) to the NLL accuracy lead only to a few percent corrections to the Born result for $A_Q(S)$. This implies that large soft-gluon contributions to the spin-dependent and unpolarized cross sections cancel each other in Eq. (3) with a good accuracy.

Therefore, contrary to the production cross sections, the single spin asymmetry in heavy flavor photoproduction is an observable quantitatively well defined in pQCD: it is stable, both parametrically and perturbatively, and insensitive to nonperturbative corrections. Measurements of the SSA in bottom photoproduction would provide an ideal test of pQCD. Data on the D-meson azimuthal distribution would make it possible to clarify the role of subleading twist contributions [10, 12].

Concerning the experimental aspects, the azimuthal asymmetry in charm photoproduction can be measured at SLAC where a coherent bremsstrahlung beam of linearly polarized photons with energies up to 40 GeV will be available soon [13]. In the approved experiments E160 and E161, charm production will be investigated using the spectra of decay muons:

$$\gamma^\uparrow + N \rightarrow c + X[\bar{c}] \rightarrow \mu^+ + X. \quad (5)$$

In this paper, we analyze the possibility to measure the SSA in heavy quark photoproduction using the decay lepton spectra. We calculate the SSA in the decay lepton azimuthal distribution:

$$\frac{d^2\sigma_\ell}{dp_{\ell T}d\varphi_\ell}(p_{\ell T}, \varphi_\ell) = \frac{1}{2\pi} \frac{d\sigma_\ell^{\text{unp}}}{dp_{\ell T}}(p_{\ell T}) [1 + A_\ell(p_{\ell T}) \mathcal{P}_\gamma \cos 2\varphi_\ell], \quad (6)$$

where φ_ℓ is the angle between the photon polarization direction and the decay lepton transverse momentum, $p_{\ell T}$. Our main results can be formulated as follows:

- The SSA transferred from the decaying c -quark to the decay muon is large in the SLAC kinematics; the ratio $A_\ell(p_T)/A_c(p_T)$ is about 90% for $p_T > 1$ GeV.
- pQCD predictions for $A_\ell(p_{\ell T})$ are also stable, both perturbatively and parametrically.
- Nonperturbative corrections to $A_\ell(p_{\ell T})$ due to the gluon transverse motion in the target and the c -quark fragmentation are small; they are about 10% for $p_{\ell T} > 1$ GeV.
- The SSA in Eq. (6) depends weakly on theoretical uncertainties in the charm semileptonic decays², $c \rightarrow \ell^+ \nu_\ell X_q$ ($q = d, s$). In particular,
 - Contrary to the the production cross sections, the asymmetry $A_\ell(p_{\ell T})$ is practically insensitive to the unobserved strange quark mass, m_s , for $p_{\ell T} > 1$ GeV.
 - The bound state effects due to the Fermi motion of the c -quark inside the D -meson have only a small impact on $A_\ell(p_{\ell T})$, in practically the whole region of $p_{\ell T}$.

We conclude that the SSA in the decay lepton azimuthal distribution (6) is also well-defined in the framework of perturbation theory and can be used as a good test of pQCD applicability to open charm production.

The paper is organized as follows. In Section 2 we analyze the properties of the decay lepton azimuthal distribution at leading order. We also give the physical explanation of the fact that pQCD predictions for the SSA are approximately the same at LO and at NLO. The details of our calculations of radiative corrections are too long to be presented in this paper; they will be reported separately in a forthcoming publication [15]. In Section 3 we discuss the nonperturbative contributions to $A_\ell(p_{\ell T})$ caused by the Peterson fragmentation, the k_T -kick and the Fermi motion of the heavy quark inside the heavy hadron. Section 4 contains experimental considerations. We discuss the conditions needed to measure the SSA at SLAC, estimate background contributions and expected errors.

² For a review see Ref. [14].

II. PQCD PREDICTIONS FOR SSA

A. Partonic Cross Sections

At the Born level, the only partonic subprocess which is responsible for the reaction (5) is the heavy quark production by photon-gluon fusion,

$$\gamma^\dagger(k_\gamma) + g(k_g) \rightarrow Q(p_Q) + \bar{Q}(p_{\bar{Q}}) \rightarrow \ell(p_\ell) + \nu_\ell + q + \bar{Q}, \quad (7)$$

with subsequent decay $c \rightarrow \ell^+ \nu_\ell q$ ($q = d, s$) in the charm case and $b \rightarrow \ell^- \bar{\nu}_\ell q$ ($q = u, c$) in the bottom one. To calculate distributions of final particles appearing in a process of production and subsequent decay, it is useful to adopt the narrow-width approximation,

$$\frac{1}{(p_Q^2 - m_Q^2)^2 + \Gamma_Q^2 m_Q^2} \rightarrow \frac{\pi}{\Gamma_Q m_Q} \delta(p_Q^2 - m_Q^2), \quad (8)$$

with Γ_Q the total width of the heavy quark. Corrections to this approximation are negligibly small in both charm and bottom cases since they have a relative size $\mathcal{O}(\Gamma_Q/m_Q)$.

In the case of the linearly polarized photon, the heavy quark produced in the reaction (7) is unpolarized. For this reason, the single-inclusive cross section for the decay lepton production in (7) is a simple convolution:

$$E_\ell \frac{d^3 \hat{\sigma}_\ell}{d^3 p_\ell}(\vec{p}_\ell) = \frac{1}{\Gamma_Q} \int \frac{d^3 p_Q}{E_Q} \frac{E_Q d^3 \hat{\sigma}_Q}{d^3 p_Q}(\vec{p}_Q) \frac{E_\ell d^3 \Gamma_{\text{sl}}}{d^3 p_\ell}(p_\ell \cdot p_Q). \quad (9)$$

At leading order, $\mathcal{O}(\alpha_{em} \alpha_s)$, the φ_Q -dependent cross section for heavy flavor production,

$$\begin{aligned} \frac{E_Q d^3 \hat{\sigma}_Q}{d^3 p_Q}(\vec{p}_Q) &\equiv \frac{2s d^3 \hat{\sigma}_Q}{du_1 dt_1 d\varphi_Q}(s, t_1, u_1, \varphi_Q) \\ &= \frac{1}{\pi s} [B_Q(s, t_1, u_1) + \Delta B_Q(s, t_1, u_1) \mathcal{P}_\gamma \cos 2\varphi_Q], \end{aligned} \quad (10)$$

is given by [10, 16]

$$B_Q(s, t_1, u_1) = \pi e_Q^2 \alpha_{em} \alpha_s \left[\frac{t_1}{u_1} + \frac{u_1}{t_1} + \frac{4m_Q^2 s}{t_1 u_1} \left(1 - \frac{m_Q^2 s}{t_1 u_1} \right) \right] \delta(s + t_1 + u_1), \quad (11)$$

$$\Delta B_Q(s, t_1, u_1) = \pi e_Q^2 \alpha_{em} \alpha_s \left[\frac{4m_Q^2 s}{t_1 u_1} \left(1 - \frac{m_Q^2 s}{t_1 u_1} \right) \right] \delta(s + t_1 + u_1), \quad (12)$$

with e_Q the quark charge in units of electromagnetic coupling constant. The corresponding partonic kinematical variables are

$$\begin{aligned} u_1 &= (k_\gamma - p_Q)^2 - m_Q^2 = -E_Q \sqrt{s} (1 - \alpha \cos \theta_Q), & s &= (k_\gamma + k_g)^2, \\ t_1 &= (k_g - p_Q)^2 - m_Q^2 = -E_Q \sqrt{s} (1 + \alpha \cos \theta_Q), & \alpha &= \sqrt{1 - m_Q^2/E_Q^2}, \end{aligned} \quad (13)$$

with θ_Q and E_Q the heavy quark polar angle and energy in the γg center-of-mass system.

At the tree level, the invariant width of the semileptonic decay $Q \rightarrow \ell \nu_\ell X_q$ can be written as

$$\frac{E_\ell d^3 \Gamma_{\text{sl}}}{d^3 p_\ell}(x) \equiv I_{\text{sl}}(x) = \frac{G_F^2 m_Q^3}{(2\pi)^4} \frac{x(1-x-\delta^2)^2}{1-x} \times \begin{cases} |V_{CKM}|^2, & Q = c \\ \frac{|V_{CKM}|^2}{6(1-x)} (3 - 2x + \delta^2 \frac{3-x}{1-x}), & Q = b \end{cases} \quad (14)$$

Here V_{CKM} denotes the corresponding element of the Cabbibo-Kobayashi-Maskawa matrix, G_F is the Fermi constant, $\delta = m_q/m_Q$ and

$$x = \frac{2(p_\ell \cdot p_Q)}{m_Q^2} = \frac{2E_\ell E_Q}{m_Q^2}(1 - \alpha \cos \theta_{\ell Q}), \quad (15)$$

where E_ℓ is the lepton energy and $\theta_{\ell Q}$ is the angle between the lepton and heavy quark momenta in the γg center-of-mass system.

To perform the angular integrations in Eq. (9), we use the cosine theorem:

$$\cos \theta_Q = \cos \theta_\ell \cos \theta_{\ell Q} - \sin \theta_\ell \sin \theta_{\ell Q} \cos \varphi_{\ell Q}, \quad (16)$$

where $\varphi_{\ell Q}$ is the azimuth of the lepton momentum in the frame where the third axis is directed along the heavy quark momentum. Substituting $d^2\Omega_Q \rightarrow d^2\Omega_{\ell Q} = d\cos \theta_{\ell Q} d\varphi_{\ell Q}$ in Eq. (9), we obtain the following master formula for the decay lepton azimuthal distribution:

$$\begin{aligned} E_\ell \frac{d^3\hat{\sigma}_\ell}{d^3p_\ell}(\vec{p}_\ell) &= \frac{1}{\pi s \Gamma_Q} \int_{\tilde{E}_Q}^{\sqrt{s}/2} |\vec{p}_Q| dE_Q \int_{\cos \tilde{\theta}_{\ell Q}}^1 d\cos \theta_{\ell Q} I_{sl}(x) \int_0^{2\pi} d\varphi_{\ell Q} \\ &\times \left[B_Q(t_1, u_1) + \left(1 - \frac{2\sin^2 \theta_{\ell Q} \sin^2 \varphi_{\ell Q}}{\sin^2 \theta_Q} \right) \Delta B_Q(t_1, u_1) \mathcal{P}_\gamma \cos 2\varphi_\ell \right], \end{aligned} \quad (17)$$

where the limits of integration are given by

$$\cos \tilde{\theta}_{\ell Q} = \max \left[-1, \frac{1}{\alpha} \left(1 - \frac{m_Q^2(1 - \delta^2)}{2E_\ell E_Q} \right) \right] \quad (18)$$

and

$$\tilde{E}_Q = \frac{m_Q}{\sqrt{1 - \max^2[\tilde{\alpha}, 0]}}, \quad \tilde{\alpha} = \frac{4E_\ell^2 - m_Q^2(1 - \delta^2)}{4E_\ell^2 + m_Q^2(1 - \delta^2)}. \quad (19)$$

Note that Eqs.(17)-(19) are applicable not only at the Born level, but also in all those cases when radiative corrections have a factorizable form (9). At the tree level, Eq.(17) can be simplified due to δ -function in the Born cross sections (10) and (11).

B. Hadron Level Results at LO

At the hadron level, the overall one-particle inclusive kinematical invariants of the reaction (5) are defined as

$$\begin{aligned} U &= (k_\gamma - p_\ell)^2 = -E_\ell \sqrt{zS}(1 - \cos \theta_\ell), & S &= (k_\gamma + p_N)^2, \\ T &= (p_N - p_\ell)^2 = -E_\ell \sqrt{S/z}(1 + \cos \theta_\ell), & k_g &= zp_N. \end{aligned} \quad (20)$$

The hadron level cross section has the form of a convolution:

$$E_\ell \frac{d^3\sigma_\ell}{d^3p_\ell}(S, T, U, \varphi_\ell) = \int_{z_m}^1 dz g(z, \mu_F) \frac{E_\ell d^3\hat{\sigma}_\ell}{d^3p_\ell}(zS, zT, U, \varphi_\ell), \quad (21)$$

in which $g(z, \mu_F)$ is the gluon distribution function and μ_F is the factorization scale. The lower limit of integration in Eq. (21) can be found from the kinematical restriction $x \leq 1 - \delta^2$. The result is:

$$z_m = \frac{4m_Q^2/S}{1 - \max^2[\beta_-, 0]}, \quad (22)$$

where

$$\beta_- = \frac{m_Q^2(1-\delta^2)}{U} \left[1 - \sqrt{\left(1 + \frac{U}{m_Q^2(1-\delta^2)}\right)^2 + \frac{4UT}{m_Q^2 S(1-\delta^2)^2}} \right]. \quad (23)$$

Experimentally, to suppress the background contributions originating from semileptonic decays of light hadrons and Bethe-Heitler process, a cut of the lepton energy in the reaction (5) is usually used [13]. For this reason, apart from the usual differential distribution,

$$\frac{d^2\sigma_\ell}{dp_{\ell T}d\varphi_\ell}(p_{\ell T}, \varphi_\ell) = \int_{p_{\ell T}}^{E_{\ell, \max}^*} \frac{E_\ell d^3\sigma_\ell}{d^3p_\ell}(S, T, U, \varphi_\ell) \frac{\lambda_- dE_\ell^*}{2\sqrt{E_\ell^{*2} - p_{\ell T}^2}}, \quad (24)$$

we consider also the quantity

$$\frac{d^2\sigma_\ell}{dp_{\ell T}d\varphi_\ell}(E_{\ell, \text{cut}}^*, p_{\ell T}, \varphi_\ell) = \int_{E_{\ell, \text{cut}}^*}^{E_{\ell, \max}^*} \frac{E_\ell d^3\sigma_\ell}{d^3p_\ell}(S, T, U, \varphi_\ell) \frac{\lambda_- dE_\ell^*}{2\sqrt{E_\ell^{*2} - p_{\ell T}^2}}. \quad (25)$$

In Eqs. (24) and (25), E_ℓ^* is the lepton energy in the lab (nucleon rest) frame,

$$E_\ell^* = \frac{m_N^2 - T}{2m_N}, \quad (26)$$

with the maximum value

$$E_{\ell, \max}^* = \frac{\sqrt{S}}{8m_N} \left(\lambda_+ \sqrt{S}(1+\beta)(1-\delta^2) + \lambda_- \sqrt{S(1+\beta)^2(1-\delta^2)^2 - 16p_{\ell T}^2} \right) \quad (27)$$

and an experimental cutoff $E_{\ell, \text{cut}}^*$; $\lambda_\pm = 1 \pm m_N^2/S$ and $\beta = \sqrt{1 - 4m_Q^2/S}$.

Let us discuss the hadron level pQCD predictions for the asymmetry in azimuthal distribution of the decay lepton. In this paper, we will discuss only the charm photoproduction at the SLAC energy $E_\gamma \approx 35$ GeV, with $E_\gamma = (S - m_N^2)/2m_N$. Unless otherwise stated, the CTEQ5M [17] parametrization of the gluon distribution function is used. The default value of the charm quark mass is $m_c = 1.5$ GeV.

Our calculations of the quantities $A_\mu(p_T)$ and $A_c(p_T)$ are given in Fig.1 by solid and dashed lines, respectively. One can see that the asymmetry transferred from the decaying c -quark to the decay muon is large in the SLAC kinematics; the ratio $A_\mu(p_T)/A_c(p_T)$ is about 90% for $p_T > 1$ GeV. Note that $p_T \equiv p_{QT}$ when we consider the heavy quark production and $p_T \equiv p_{\ell T}$ when the quantity $A_\mu(p_{\ell T})$ is discussed.

In Fig. 2 we show the LO predictions for $A_\mu(p_T)$ at different values of the cutoff parameter $E_{\ell, \text{cut}}^*$. One can see that, contrary to the production cross sections, the SSA depends weakly on $E_{\ell, \text{cut}}^*$ over practically the whole region of p_T . This property of $A_\mu(p_T)$ will be especially useful in interpretation of data. In Fig. 3 we show the SSA, $A_\mu(p_T)$, in different intervals of the muon energy E_ℓ^* .

The most interesting property of the azimuthal asymmetry, closely related to fast perturbative convergence, is its parametric stability³. As was shown in [10], the LO predictions for $A_Q(p_T)$ are insensitive (to within few percent) to standard theoretical uncertainties in the QCD input parameters: μ_R , μ_F , Λ_{QCD} and in the gluon distribution function. We have verified that the same situation takes place in the case of decay leptons too. In particular, all the CTEQ5 versions of the gluon density, as well as the MRST [18] parametrizations, lead to predictions for $A_\mu(p_T)$ that coincide with each other with an accuracy of better than 1-2%.

³ Of course, parametric stability of the fixed-order results does not imply a fast convergence of the corresponding series. However, a fast convergent series must be parametrically stable. In particular, it must be μ_R - and μ_F -independent.

The main source of uncertainties in the LO predictions for both $A_c(p_T)$ and $A_\mu(p_T)$ is the charm quark mass. The dependence of p_T -spectra on the variation of m_c is shown in Fig. 4 and Fig. 5 for $A_c(p_T)$ and $A_\mu(p_T)$, respectively. One can see that changes of the charm quark mass in the interval $1.3 < m_c < 1.7$ GeV affect the quantity $A_c(p_T)$ by less than 20% at $p_T < 2.5$ GeV. Analogous changes of m_c lead to 20% variations of $A_\mu(p_T)$ at $1 < p_T < 2.5$ GeV.

We have also analyzed the dependence of the SSA in the lepton distribution on the unobserved strange quark mass, m_s . Fig. 5 shows that the LO predictions for $A_\mu(p_T)$ are practically independent of $\delta = m_s/m_c$ at $p_T > 1$ GeV.

C. Radiative Corrections

In Ref. [11], radiative corrections to the SSA in heavy quark production by linearly polarized photons have been investigated in the soft-gluon approximation. The calculations show that the azimuthal asymmetry in both charm and bottom production is practically insensitive to the soft-gluon corrections at energies of the fixed target experiments. This implies that large soft-gluon contributions to the spin-dependent and unpolarized cross sections cancel each other in Eq. (3) with a good accuracy. One can assume that the same situation takes place for the azimuthal asymmetry in the decay lepton distribution.

Our calculations of the factorizable NLO corrections to $A_\mu(p_T)$ show that this is really the case. We have computed both spin-dependent and unpolarized differential distributions (10) of the heavy-quark photoproduction at NLO to the next-to-leading logarithmic accuracy. The NLO corrections to the width of the heavy quark semileptonic decays are known exactly [19, 20]. We have found that radiative corrections to the leptonic SSA, $A_\mu(p_T)$, in the reaction (5) are of the order of 1% in the SLAC kinematics.

Two main reasons are responsible for perturbative stability of the quantity $A_\mu(p_T)$. First, radiative corrections to the SSA in heavy quark production are small [11]. Second, the ratio $I_{\text{sl}}^{\text{NLO}}(x)/I_{\text{sl}}^{\text{Born}}(x)$ is a constant practically at all x , except for a narrow endpoint region $x \approx 1$ [20]. (Note that $I_{\text{sl}}^{\text{Born}}(x)$ is the LO invariant width of the semileptonic decay $c \rightarrow \ell^+ \nu_\ell X_q$ given by (14) while $I_{\text{sl}}^{\text{NLO}}(x)$ is the corresponding NLO one.) The details of our NLO analysis are too long to be presented here and will be given in a separate publication [15].

III. NONPERTURBATIVE CONTRIBUTIONS

Let us discuss how the pQCD predictions for single spin asymmetry are affected by nonperturbative contributions due to the intrinsic transverse motion of the gluon and the hadronization of the produced heavy quark. Because of the relatively low c -quark mass, these contributions are especially important in the description of the cross section for charmed particle production [1]. At the same time, our analysis shows that nonperturbative corrections to the single spin asymmetry are not large.

A. Fragmentation

Hadronization effects in heavy flavor production are usually modeled with the help of the Peterson fragmentation function [21],

$$D(y) = \frac{a_\varepsilon}{y [1 - 1/y - \varepsilon/(1 - y)]^2}, \quad (28)$$

where a_ε is a normalization factor and $\varepsilon_D = 0.06$ in the case of a D -meson production. The double differential distribution of a heavy meson has the form

$$\frac{d^2\sigma_D}{dp_{DT}d\varphi_Q}(\vec{p}_{DT}) = \int_{y_m}^1 \frac{dy}{y} D(y) \frac{d^2\sigma_Q}{dp_{QT}d\varphi_Q}(\vec{p}_{DT}/y), \quad (29)$$

where $\frac{d^2\sigma_Q}{dp_{QT}d\varphi_Q}$ is the inclusive spectrum of the reaction (1) and $y_m = \frac{2p_{DT}}{\beta\sqrt{S}}$.

Our calculations of the asymmetry in a D -meson production at LO with and without the Peterson fragmentation effect are presented in Fig. 6 by dotted and solid curves, respectively. For $p_{DT} \geq 1$ GeV the fragmentation corrections to $A_c(p_T)$ are less than 10%.

Analogous corrections to the asymmetry in the decay lepton azimuthal distribution, $A_\mu(p_T)$, are given in Fig. 7. One can see that the effect of the fragmentation function (28) is practically negligible in the whole region of $p_{\ell T}$.

B. k_T Smearing

To introduce k_T degrees of freedom, $\vec{k}_g \simeq z\vec{k}_N + \vec{k}_T$, one extends the integral over the parton distribution function in Eq. (21) to k_T -space,

$$dzg(z, \mu_F) \rightarrow dzd^2k_T f(\vec{k}_T) g(z, \mu_F). \quad (30)$$

The transverse momentum distribution, $f(\vec{k}_T)$, is usually taken to be a Gaussian:

$$f(\vec{k}_T) = \frac{e^{-k_T^2/\langle k_T^2 \rangle}}{\pi\langle k_T^2 \rangle}. \quad (31)$$

In practice, an analytic treatment of k_T effects is usually used. According to [22], the k_T -smeared differential cross section of the process (1) is a 2-dimensional convolution:

$$\frac{d^2\sigma_Q^{\text{kick}}}{dp_{QT}d\varphi_Q}(\vec{p}_{QT}) = \int d^2k_T \frac{e^{-k_T^2/\langle k_T^2 \rangle}}{\pi\langle k_T^2 \rangle} \frac{d^2\sigma_Q}{dp_{QT}d\varphi_Q}\left(\vec{p}_{QT} - \frac{1}{2}\vec{k}_T\right). \quad (32)$$

The factor $\frac{1}{2}$ in front of \vec{k}_T in the r.h.s. of Eq. (32) reflects the fact that the heavy quark carries away about one half of the initial energy in the reaction (1).

Values of the k_T -kick corrections to the asymmetry in the charm production, $A_c(p_T)$, are shown in Fig. 6 by dashed ($\langle k_T^2 \rangle = 0.5$ GeV²) and dash-dotted ($\langle k_T^2 \rangle = 1$ GeV²) curves. One can see that k_T -smearing is important only in the region of relatively low $p_{QT} \leq m_c$. Note also that the fragmentation and k_T -kick effects practically cancel each other in the case of $\langle k_T^2 \rangle = 0.5$ GeV².

Corresponding calculations for the case of the lepton asymmetry are presented in Fig. 7. It is seen that $A_\mu(p_T)$ is affected by k_T -corrections systematically less than $A_c(p_T)$.

C. Fermi Motion

The third type of nonperturbative corrections we considered can be associated with the motion of the heavy quark inside the produced (and decaying) hadron; they are commonly referred to as Fermi motion. These effects are included in the heavy-quark expansion by resumming an infinite set of leading-twist corrections into a shape function $F(k_+)$, where $k_+ = k_0 + k_3$ is the positive light cone component of the heavy quark residual momentum inside the heavy meson [23, 24]. The physical decay distributions, $d\Gamma_{\text{sl}}^{(\text{H})}$, are obtained from a convolution of parton model spectra, $d\Gamma_{\text{sl}}^{(\text{Q})}$, with this function. This convolution is such that, in the perturbative formula for the decay distribution, the heavy quark mass is replaced by the momentum-dependent mass $m^* = m_Q + k_+$ [25]:

$$E_\ell \frac{d^3\Gamma_{\text{sl}}^{(\text{H})}}{d^3p_\ell}(M_H, x_H) = \int_{x_H M_H}^{M_H} \frac{E_\ell d^3\Gamma_{\text{sl}}^{(\text{Q})}}{d^3p_\ell}\left(m^*, x_H \frac{M_H}{m^*}\right) F(m^*) dm^*. \quad (33)$$

The parton-level width, $d^3\Gamma_{\text{sl}}^{(\text{Q})}(m_Q, x)$, in the r.h.s of Eq.(33) is defined by Eq. (14), M_H is the heavy meson mass and the hadron level variable x_H is related to $x = 2(p_\ell \cdot p_Q)/m_Q^2$ by $x_H = xm_Q/M_H$.

Some of the properties of $F(k_+)$ are known. The first three moments satisfy $\Lambda_0 = 1$, $\Lambda_1 = 0$ and $\Lambda_2 = \frac{1}{3}\mu_\pi^2$, where μ_π^2 is the average momentum squared of the heavy quark inside the heavy meson and the moments are defined by $\Lambda_n = \langle k_+^n \rangle = \int_{-m_Q}^{\bar{\Lambda}} dk_+ k_+^n F(k_+)$ with $\bar{\Lambda} = M_H - m_Q$. In our calculations we use a simple two-parametric model [25]:

$$F(k_+) = N e^{(1+a)\eta} (1-\eta)^a; \quad \eta = \frac{k_+}{\bar{\Lambda}}, \quad (34)$$

where the condition $\Lambda_0 = 1$ fixes the normalization factor N and the parameter a is related to the second moment as $\Lambda_2 = \frac{1}{3}\mu_\pi^2 = \bar{\Lambda}^2/(1+a)$.

Our predictions for the asymmetry $A_\mu(p_T)$ at different values of μ_π^2 and $\bar{\Lambda}$ are give in Fig. 8. One can see that the bound state effects due to the Fermi motion of the heavy quark inside the heavy hadron are small in the whole region of $p_{\ell T}$. Taking into account that $A_\mu(p_T)$ is also practically independent of m_s at $p_{\ell T} \geq 1$ GeV, we conclude that our predictions for the SSA in secondary lepton distribution are insensitive to the theoretical uncertainties in description of the charm semileptonic decays [14].

IV. EXPERIMENTAL CONSIDERATIONS

The conditions needed to measure the SSA in open charm photoproduction are:

- a high intensity photon beam with energy above 30 GeV,
- a high degree of linear polarization, and
- a large acceptance spectrometer.

These conditions are similar to those of the approved E161 experiment [13] at SLAC, in which circularly polarized photons impinging on longitudinally polarized nucleons will be used to study $\Delta G(x)$ via open charm production. To measure the SSA under consideration, target polarization is not needed, so the microwaves that polarize the planned LiD target can be turned off. Linearly polarized photons can be obtained with an appropriate choice of the diamond used to produce coherent bremsstrahlung. Two orientations of linear polarization are obtained by rotating the diamond. The SSA can be measured using high p_T muons in the E161 spectrometer, with cuts that minimize backgrounds.

A. Photon Beam

The most important difference from E161 is the change from circular to linear polarization. The E161 experiment plans to use coherent bremsstrahlung from a diamond target to produce polarized photons. Longitudinally polarized electrons are needed for circular polarization, which is largest for large values of E_γ/E_e , where E_e is the incident electron beam energy, and E_γ is the resulting photon beam energy. To obtain linear polarization, the electrons can be unpolarized, and the extent of linear polarization is largest for low values of E_γ/E_e . For a fixed photon energy, it is therefore essential to use the highest possible value of E_e , which is about 50 GeV at SLAC. Traditionally, thin diamonds and a high degree of photon collimation are used to enhance the ratio of coherent to incoherent photons, and hence the effective polarization. To obtain a sufficient flux of photons at SLAC, it is necessary to use a relatively thick diamond (we choose 1.5 mm), and a modest collimation angle of $35 \mu\text{r}$, which is several times the characteristic bremsstrahlung angle $m_e/E_e \approx 10 \mu\text{r}$. The photon intensity and the degree of linear polarization for a diamond orientation that produces a primary peak from the $(02\bar{2})$ inverse lattice point at 35 GeV are shown in Fig. 9 for the emittance and maximum intensity conditions of the SLAC electron beam. Calculations were done using a Monte Carlo simulation based on the formulas of Ref. [26]. The flux in the region 30 to 35 GeV is about 10^{10} photons/sec. The linear polarization peaks at about 0.4, with an average value of about 0.2 in the 30 to 35 GeV region. Contributions from the higher energy peaks (from the $(04\bar{4})$, $(06\bar{6})$, etc. inverse lattice points) will be small because both the flux and polarization are considerably reduced compared to the primary coherent peak.

B. Open Charm Detection and Backgrounds

Because of the poor duty factor at SLAC, simulations made for E161 have shown that the best signal-to-background ratio is obtained by tagging open charm with one or more high transverse momentum muons. In the case of the SSA, the asymmetry rises rapidly with p_T , then becomes roughly constant for $p_T > 1$ GeV. All background processes except J/ψ decay decrease more rapidly with p_T than open charm (as discussed in more detail below), therefore measuring at the highest possible p_T will optimize signals over backgrounds. However, the open charm cross section decreases with p_T , which reduces statistical accuracy. The best compromise is for p_T values centered at 1 GeV.

The most significant background process generating single muon with high p_T is the decay of pions and kaons. This was simulated using PYTHIA [27] for typical photoproduction events that were allowed to decay in a block of copper placed close to the target. Studies using GEANT indicate that an effective path length before pions and kaons are absorbed is 50 cm of copper, so this was used as the effective decay length. The rates from π, K decays are shown as the diamonds in Fig. 10 for any sign muon with $7.5 < E_\mu^* < 10$ GeV. They are compared with the rate of muons predicted from open charm decay as calculated using the photon-gluon fusion process in PYTHIA, scaled by a factor of two to match experimental data. The π, K decay background is lower for negative muons than for positive muons by typically 50%, so one sign will be easier to measure than the other. The rate and SSA for π, K decay muons can be measured by moving the copper absorber a significant distance from the target, thus doubling or tripling the decay rates. Measurements can also be made for $5 < E_\mu^* < 7.5$ GeV, with somewhat larger relative backgrounds from π, K decays. In the interesting range $0.8 < p_T < 1.2$ GeV, π and K decays become dominant below $E_\mu^* \approx 4$ GeV, making experimental measurements difficult in this energy region.

Another significant process is wide-angle muon pair production from the target nuclei (Li and D). The rates calculated using Ref. [28] are shown as the crosses in Fig. 10. The rates are for events in which only one of the two muons from the Bethe-Heitler pair is detected in the proposed E161 spectrometer. Events in which both muons would be detected can be vetoed in the data analysis, reducing the Bethe-Heitler background by about a factor of two. The remaining background is well below the open charm rate. It can be calculated quite accurately, and reliable corrections applied to the data.

Backgrounds from the decay of vector mesons are relatively unimportant for $p_T \approx 1$ GeV, and can be measured using the approximately 50% of events in which both muons are detected in the spectrometer.

The final background is from J/ψ decay, for which the typical p_T peaks around 1.5 GeV. Fortunately, most of the time the second muon is detected in the E161 spectrometer, so the background only becomes large for $p_T > 1.3$ GeV and $E_\mu^* > 10$ GeV, and can be measured using the large sample of events in which both muons are detected.

In summary, in the optimal case of negative muons with $7.5 < E_\mu^* < 10$ GeV and $p_T > 0.9$ GeV, the signal-to-background ratio is estimated to be about 3:1, leading to an effective dilution factor of about 1.3, equivalent to a factor of 1.6 more running time than is needed in the absence of backgrounds. This estimate relies crucially on the open charm cross section as a function of p_T , which is poorly known at present (factor of two uncertainties). Thus, the relative background situation could be better or worse, depending on what open charm cross sections are measured in the experiment.

C. Projected Errors

The cross section for producing negative muons from open charm decays with $7.5 < E_\mu^* < 10$ GeV and $p_T > 0.9$ GeV is approximately 0.2 to 0.5 nb at $E_\gamma = 35$ GeV, as estimated using the PYTHIA Monte Carlo. If we assume the E161 luminosity, i.e. a flux of 10^{10} photons per second, a 1.6 gm/cm² target, and a spectrometer acceptance of about 50% for the events of interest, the open charm rate is of order 100,000 events per day. For an average linear polarization of 0.2, a statistical error of about 0.02 on the SSA would be obtained in one day of running. This error bar is sufficient to make a good test of the QCD predictions, and further improvements to the statistical error would be soon be lost in the estimated 10% (relative) systematics error, dominated by the uncertainty in the linear polarization. With about a factor of four larger running time, measurements with an error of about 0.02 could be separately made of positive and negative muons, and in several bins of E_μ^* spanning $5 < E_\mu^* < 20$ GeV.

This would be very useful in testing the assumed dominance of the photon-gluon fusion mechanism. A difference in positive and negative muon results might indicate contributions from soft associated production processes, while high- x_F behavior of the SSA can be sensitive to diffractive contributions [10]. Approximately the same running time would be needed for 25 GeV incident photons as for $E_\gamma = 35$ GeV, because the lower charm cross section and higher backgrounds would be compensated for by higher photon linear polarization.

V. CONCLUSION

In this paper we analyze the possibility to measure the SSA in open charm photoproduction in the E160/E161 experiments at SLAC where a coherent bremsstrahlung beam of linearly polarized photons with energies up to 40 GeV will be available soon. In these experiments, charm production will be investigated with the help of inclusive spectra of secondary muons. The SSA transferred from the decaying c -quark to the decay muon is predicted to be large for SLAC kinematics; the ratio $A_\ell(p_T)/A_c(p_T)$ is about 90% at $p_T > 1$ GeV. Our calculations show that the SSA in decay lepton distribution preserves all remarkable properties of the SSA in heavy flavor production: it is stable, both perturbatively and parametrically, and practically insensitive to nonperturbative contributions due to the gluon transverse motion in the target and heavy quark fragmentation. We have also found that QCD predictions for $A_\ell(p_T)$ depend weakly on theoretical uncertainties in the charm semileptonic decays. We conclude that measurements of $A_\ell(p_T)$ in the E160/E161 experiments would provide a good test of pQCD applicability to open charm production.

Note also that because of the low c -quark mass, the power corrections to the charm production can be essential. As was shown in [10], the pQCD and Regge approaches lead to strongly different predictions for the single spin asymmetry in the region of low p_T and large Feynman x_F . Data on the p_T - and x_F -distributions of the SSA in D -meson photoproduction could make it possible to discriminate between these mechanisms.

Acknowledgements. We would like to thank S.J. Brodsky, A. Capella, E. Chudakov, L. Dixon, A.B. Kaidalov, A.E. Kuraev, M.E. Peskin and A.V. Radyushkin for useful discussions. N.Ya.I. is grateful to Theory Groups of SLAC and JLab for hospitality while this work has been completed. This work was supported in part by the National Science Foundation.

-
- [1] S. Frixione, M.L. Mangano, P. Nason and G. Ridolfi, hep-ph/9702287, published in "Heavy Flavours II", eds. A.J. Buras and M. Lindner, Advanced Series on Directions in High Energy Physics (World Scientific Publishing Co., Singapore, 1998).
 - [2] M.L. Mangano, P. Nason and G. Ridolfi, Nucl. Phys. **B373** (1992), 295.
 - [3] S. Frixione, M.L. Mangano, P. Nason and G. Ridolfi, Nucl. Phys. **B412** (1994), 225.
 - [4] N. Kidonakis, Int. J. Mod. Phys. **A15** (2000), 1245.
 - [5] E. Laenen, J. Smith and W.L. van Neerven, Nucl. Phys. **B369** (1992), 543.
 - [6] E.L. Berger and H. Contopanagos, Phys. Rev. **D 54** (1996), 3085.
 - [7] S. Catani, M.L. Mangano, P. Nason and L. Trentadue, Nucl. Phys. **B478** (1996), 273.
 - [8] N. Kidonakis, Phys. Rev. **D64** (2001), 014009.
 - [9] H. Lai and H. Li, Phys. Lett. **B471** (1999), 220.
 - [10] N.Ya. Ivanov, A. Capella and A.B. Kaidalov, Nucl. Phys. **B586** (2000), 382.
 - [11] N.Ya. Ivanov, Nucl. Phys. **B615** (2001), 266.
 - [12] S.J. Brodsky, E. Chudakov, P. Hoyer and J.M. Laget, Phys. Lett. **B498** (2001), 23.
 - [13] SLAC E161, (2000), <http://www.slac.stanford.edu/exp/e160>.
 - [14] B. Blok, R. Dikeman and M. Shifman, Phys. Rev. **D51** (1995), 6167.
 - [15] N.Ya. Ivanov, Nucl. Phys. **B666** (2003), 88.
 - [16] A.D. Watson, Zeit. Phys. **C12** (1982), 123.
 - [17] H.L. Lai *et al.*, Eur. Phys. J. **C12** (2000), 375.
 - [18] A.D. Martin, R.G. Roberts, W.J. Stirling and R.S. Thorne, Eur. Phys. J. **C4** (1998), 463.
 - [19] A. Ali and E. Pietarinen, Nucl. Phys. **B154** (1979), 519.

- [20] M. Jeřabek and J.H. Kühn, Nucl. Phys. **B320** (1989), 20.
- [21] C. Peterson, D. Schlatter, I. Schmitt and P. Zerwas, Phys. Rev. **D 27**(1983), 105.
- [22] L. Apanasevich, C. Balazs, C. Bromberg *et al.*, Phys. Rev. **D59** (1999), 074007.
- [23] I.I. Bigi, M.A. Shifman, N.G. Uraltsev and A.I. Vainshtein, Int. J. Mod. Phys. **A9** (1994), 2467; Phys. Lett. **B328** (1994), 431.
- [24] M. Neubert, Phys. Rev. **D49** (1994), 3392; Phys. Rev. **D49** (1994), 4623.
- [25] F. De Fazio and M. Neubert, JHEP **06** (1999), 017.
- [26] G. Diambrini Palazzi, Rev. Mod. Phys. **40** (1968), 611.
- [27] T. Sjostrand, Computer Physics Commun. **82** (1994), 74.
- [28] Y.S. Tsai, Rev. Mod. Phys. **46** (1974), 815; Rev. Mod. Phys. **49** (1977), 421 (E).

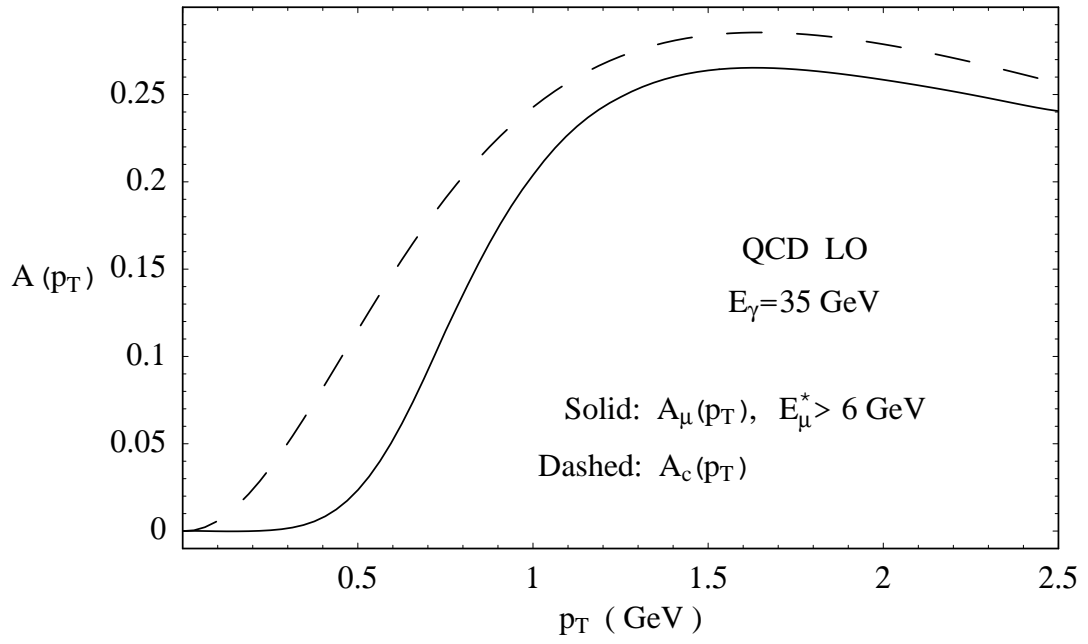


FIG. 1: Comparison of the QCD LO predictions for $A_\mu(p_T)$ and $A_c(p_T)$.

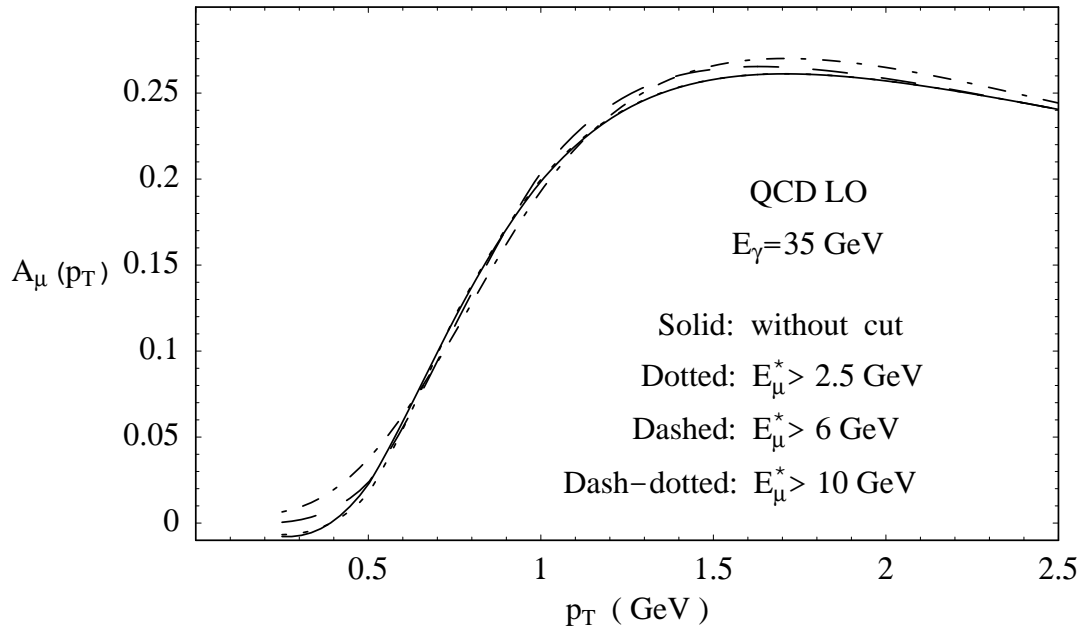


FIG. 2: Dependence of the leptonic SSA, $A_\mu(p_T)$, on the cutoff parameter $E_{\mu,\text{cut}}^*$.

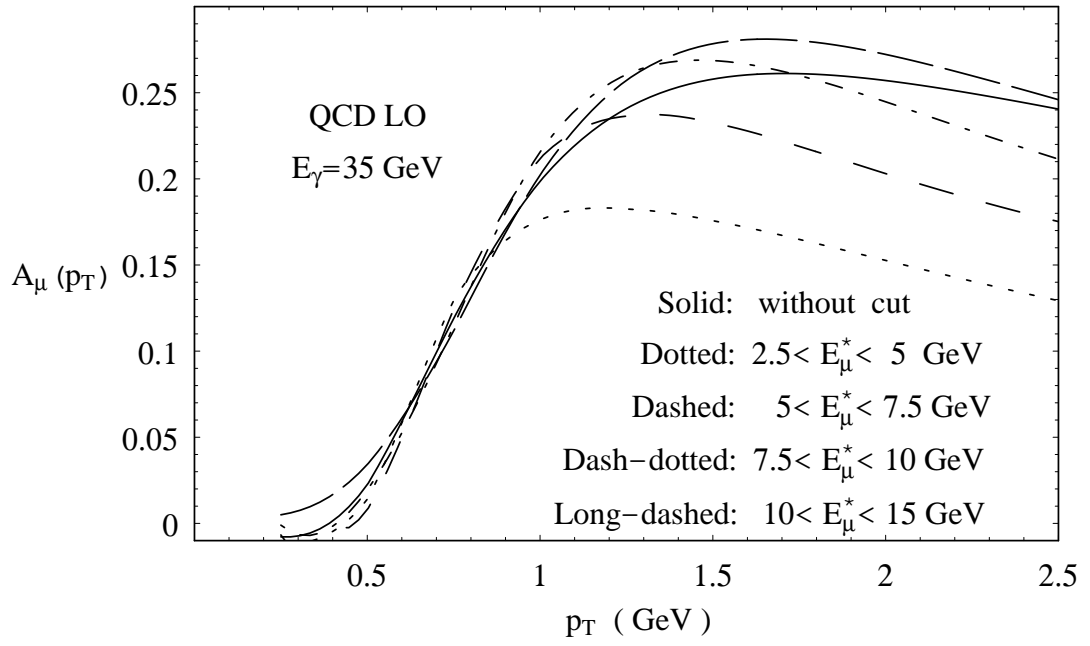


FIG. 3: SSA, $A_\mu(p_T)$, in different intervals of the lepton energy E_μ^* .

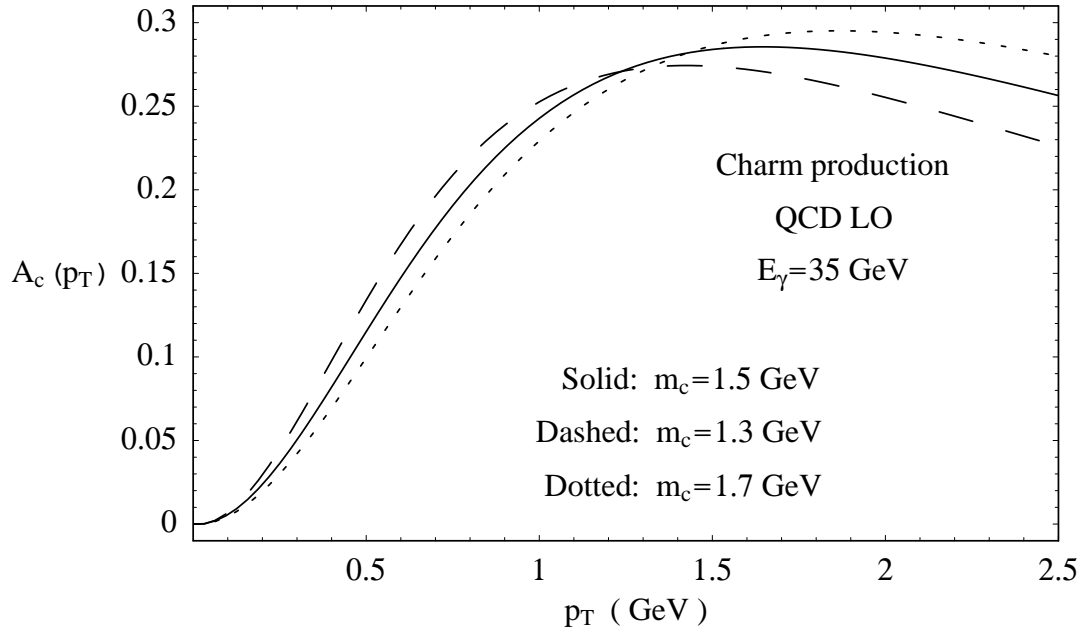


FIG. 4: Dependence of the SSA in charm production, $A_c(p_T)$, on the c -quark mass, m_c .

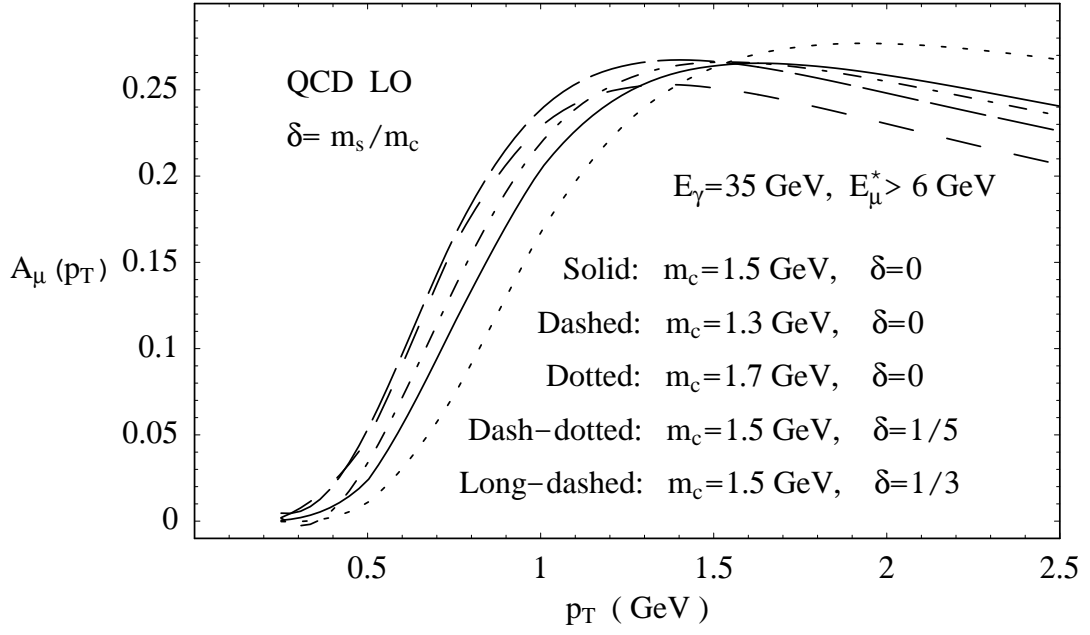


FIG. 5: Dependence of the leptonic SSA, $A_\mu(p_T)$, on the charm and strange quark mass, m_c and m_s .

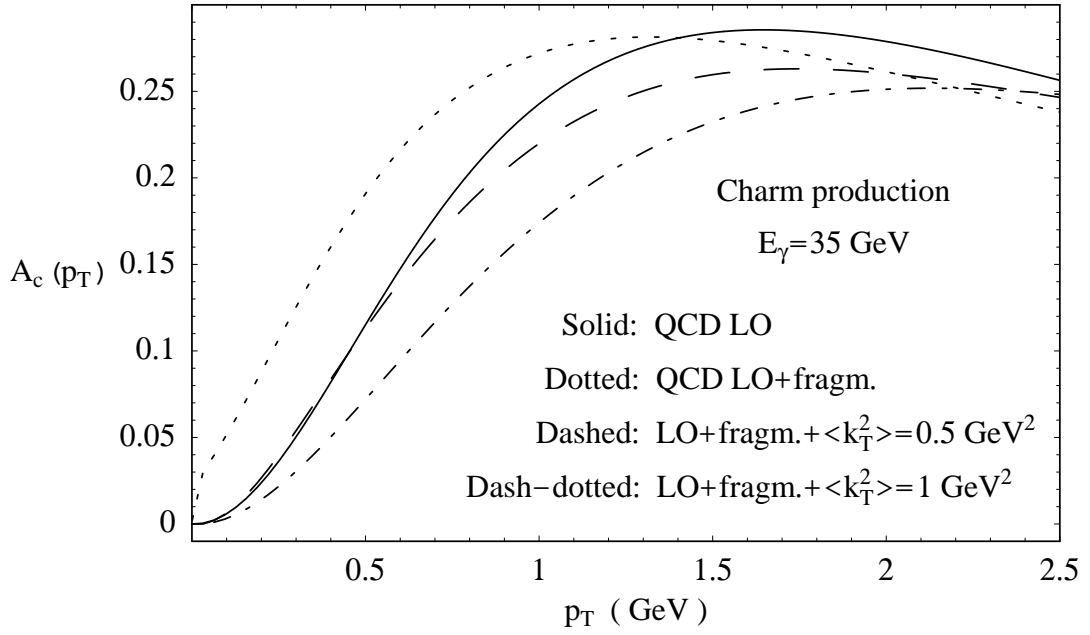


FIG. 6: SSA in a D -meson production; the QCD LO predictions with and without the inclusion of the k_T smearing and Peterson fragmentation effects.

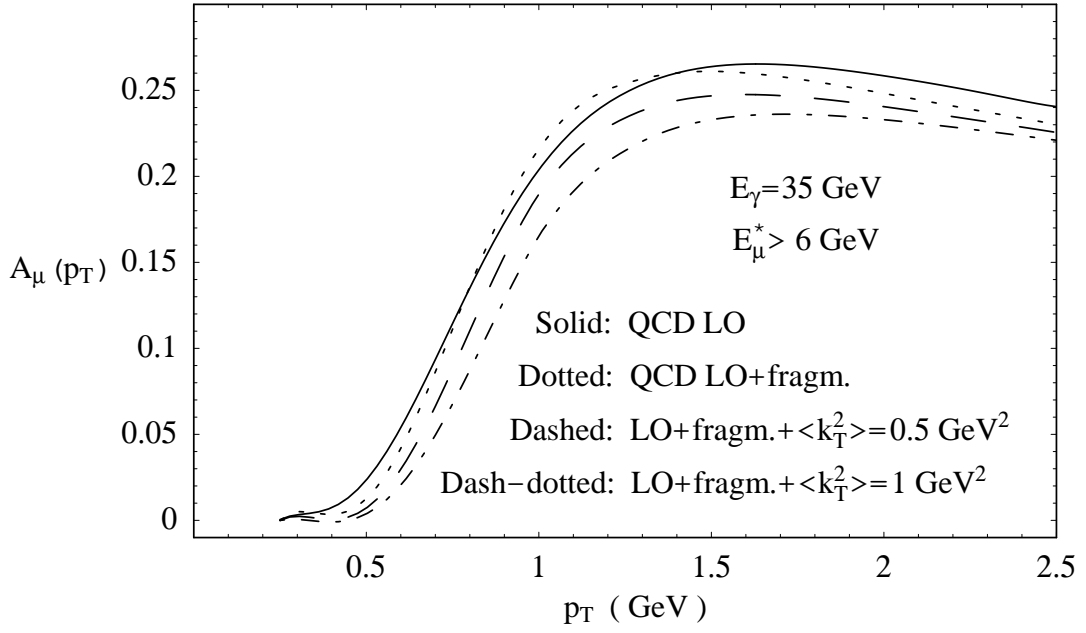


FIG. 7: SSA, $A_\mu(p_T)$, in the decay lepton distribution; the QCD LO predictions with and without the inclusion of the k_T smearing and Peterson fragmentation effects.

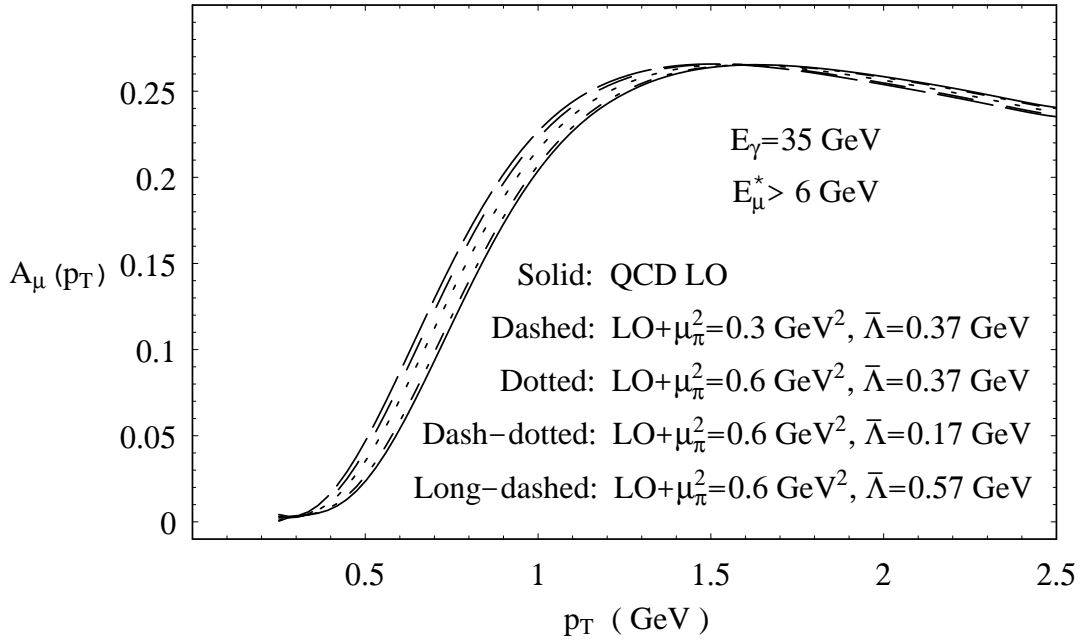


FIG. 8: Fermi motion corrections to the leptonic SSA, $A_\mu(p_T)$, at different values of μ_π^2 and $\bar{\Lambda}$.

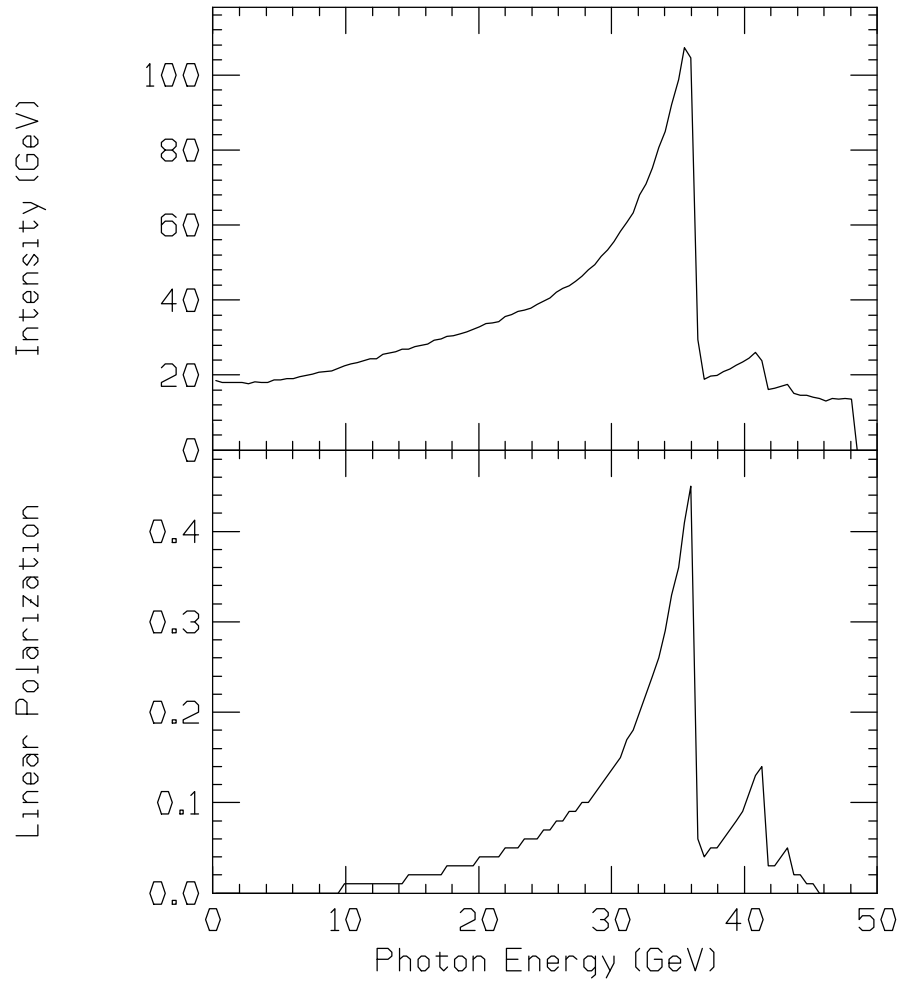


FIG. 9: The upper panel shows the predicted relative intensity of photons (intensity is energy-weighted flux) for coherent bremsstrahlung with a primary coherent peak at $E_\gamma = 35$ GeV. The lower panel shows the calculated linear polarization under conditions typical of SLAC E161.

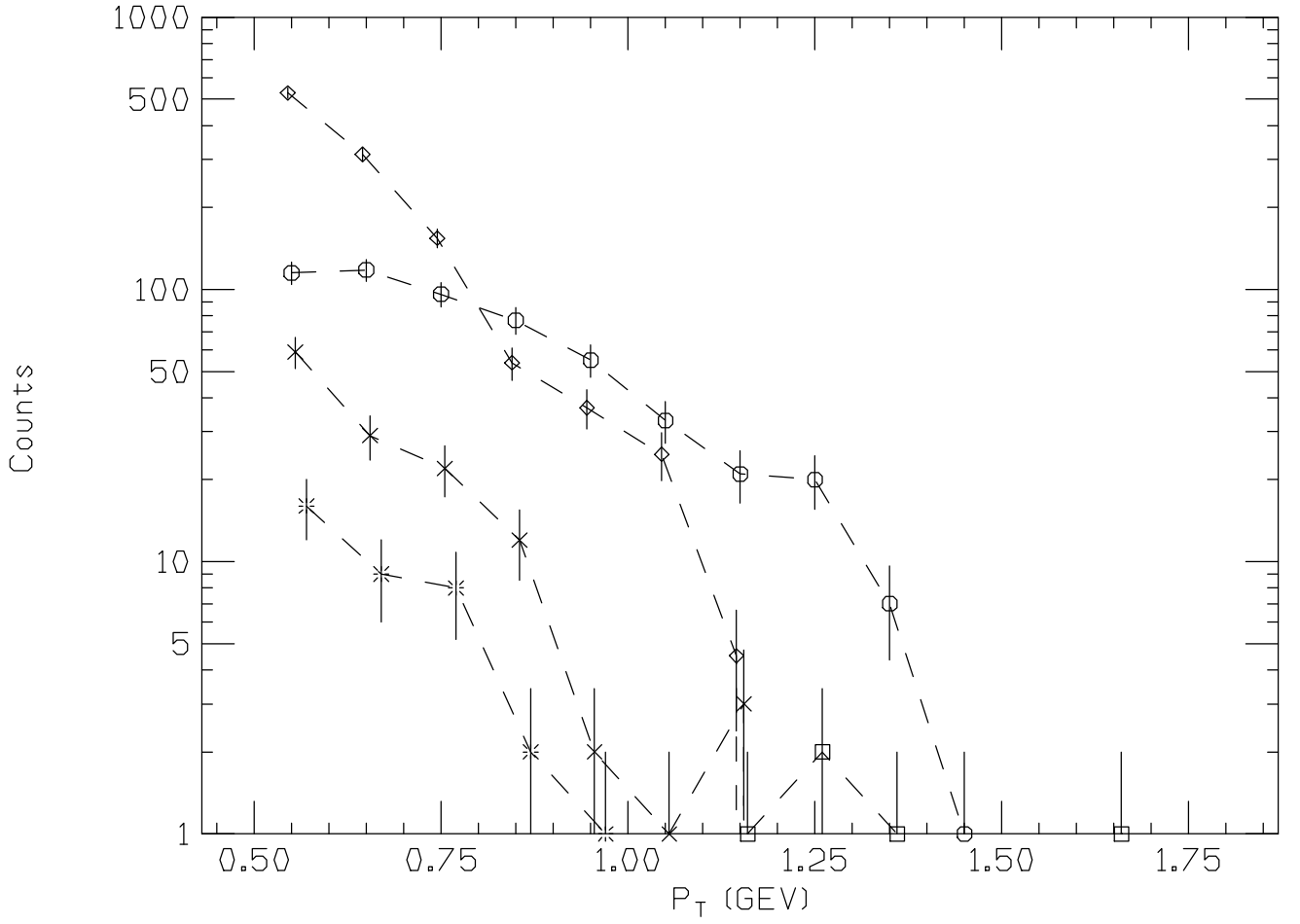


FIG. 10: Relative number of counts from open charm (circles), pion and kaon decays (diamonds), nuclear pair production (crosses), light vector meson decays (stars), and J/ψ decays (boxes), for $7.5 < E_\mu^* < 10$ GeV as a function of p_T for $30 < E_\gamma < 35$ GeV. The count rates correspond to about one minute under E161 conditions.